ANALYSIS OF A REGIONAL SCALE CHEMICAL-TRANSPORT MODEL TO INVESTIGATE THE POTENTIONAL CAPABILTY OF SATELLITES FOR IDENTIFYING A WIDESPREAD AIR POLLUTION EVENT

Jason R. Welsh and Jack Fishman*

Department of Earth and Atmospheric Sciences, Saint Louis University, St. Louis MO 63108 USA

* Correspondence: jfishma2@slu.edu

Abstract: We use a regional scale photochemical transport model to investigate the surface concentrations and column integrated amounts of ozone (O_3) and nitrogen dioxide (NO_2) during a pollution event that occurred in the St. Louis metropolitan region in 2012. These trace gases will be two of the primary constituents that will be measured by TEMPO, an instrument on a geostationary platform, which will result in a dataset that has hourly temporal resolution during the daytime and ~4 km spatial resolution.   Although air quality managers are most concerned with surface concentrations, satellite measurements provide a quantity that reflects a column amount, which may or may not be directly relatable to what is measured at the surface.   The model results provide good agreement with observed surface O_3 concentrations, which is the only trace gas dataset that can be used for verification.   The model shows that a plume of O_3 extends downwind from St. Louis and contains an integrated amount of ozone of ~ 16 DU (1 DU = 2.69×10^{16} mol. cm^{-2}), a quantity that is two to three times lower than what was observed by satellite measurements during two massive pollution episodes in the 1980s.   Based on the smaller isolatable emissions coming from St. Louis, this quantity is not unreasonable, but may also reflect the reduction of photochemical ozone production due to the implementation of emission controls that have gone into effect in the past few decades.

Keywords: tropospheric ozone; pollution episode; satellite measurements; regional transport

I. Introduction

*1a. Overview*

More than three decades have passed since Fishman et al. (1987) showed that air pollution information could be inferred from solar backscattered ultraviolet radiation measurements from satellite sensors. That study identified a synoptic-scale ozone pollution event that evolved over several days and illustrated how enhanced surface ozone observations were embedded within total ozone measurements made by the TOMS (Total Ozone Mapping Spectrometer) instrument.   In subsequent studies, Fishman et al. (1990; 2003) provided a methodology that was able to separate tropospheric ozone from the total ozone column using independent concurrent measurements from other instruments such as SAGE (Stratospheric Aerosol Gas Experiment) and SBUV (Solar Backscatter Ultraviolet), which were used to construct stratospheric ozone profiles.   These stratospheric ozone profiles were then subtracted from the TOMS total ozone amounts to produce a quantity known as tropospheric ozone residual (TOR).   Similarly, the use of concurrent total ozone quantities from OMI (Ozone Monitoring Instrument) and stratospheric ozone profiles derived from the MLS (Microwave Limb Scanning) instruments aboard the Aura satellite launched in 2004 have provided an impressive dataset, which Ziemke et al. (1998; 2006) and Levelt et al. (2017) define as tropospheric column ozone (TCO).   Both the TOR and TCO have provided valuable insight into the global distribution of the amount of ozone in the troposphere, and especially how these distributions

relate to the use of fossil fuel in the northern hemisphere and widespread biomass burning in the tropics.

With respect to their use for air pollution studies, measurements from OMI, multiple versions of the GOME (Global Ozone Monitoring Experiment), and the SCIAMACHY (acronym) instruments have provided nitrogen dioxide (NO_2) column measurements that clearly show the distribution of the emissions on scales of only a few kilometers (e.g., Russell et al., 2012; Duncan et al., 2016). Using these measurements, which are obtained through the application of the DOAS (Differential Optical Absorption Spectroscopy) retrieval methodology (Platt and Stutz, 2008) to these backscattered UV measurements, numerous studies show well-defined spatial emission patterns within urban areas, weekday-vs.-weekend differences in major cities, and perhaps most significantly, long-term trends in NO_2 emissions, which highlight the impact of regulations imposed on them since the early 2000s (Duncan et al., 2016).

However, the challenge remains defining a direct measurement relationship between what is observed from satellites, which is a column measurement, and what is observed at the surface, which, from an air quality manager's perspective, is generally the quantity that most often determines whether or not a region meets National Ambient Air Quality Standards (NAAQS; https://www.epa.gov/criteria-air-pollutants/naaqs-table) criteria for determining whether or not a specific region is in compliance with the NAAQS. Relationships between NO_2 emissions and satellite-derived inferred emissions have been studied and shown to be in good agreement (see Figure 1, from Lu et al., 2015). On the other hand, *in situ* surface NO_2 measurements are not plentiful enough and suffer from frequent concentrations below instrumental detection limits that they are difficult to compare with satellite observations. In addition, it is extremely rare if an urban area is in violation of the NAAQS NO_2 standard, so there is generally not a significant need to have the space-based measurements as a potential alternative measurement technique.
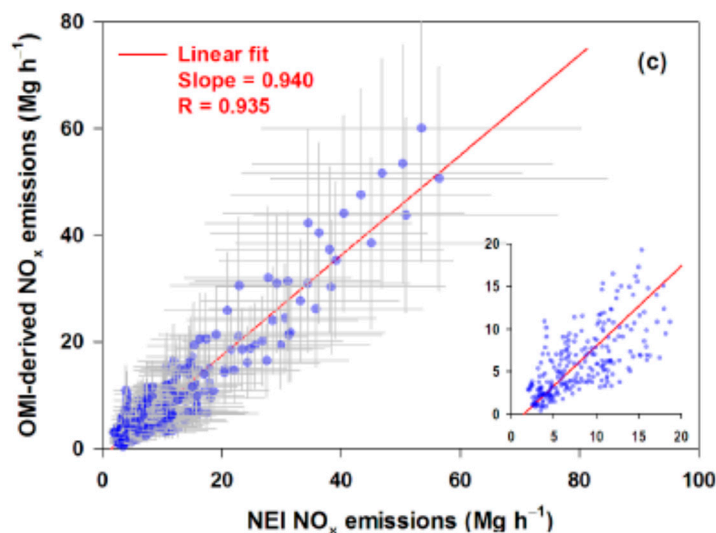
Figure 1. Comparison of satellite-derived and bottoms-up emissions estimates (from Lu et al., 2015)

Ground level ozone is the NAAQS pollutant that is most frequently in violation of the standard (NAS,1991;https://www.uschamber.com/issue-brief/ozone-national-ambient-air-quality-standards#ozone_problems), but there have been only a couple of studies that relate TOR or TCO satellite-derived measurements to *in situ* O_3 concentrations. For validation, TOR and TCO are compared with ozonesonde measurements (e.g., Fishman et al., 1990; Fishman and Balok, 1999; Ziemke et al., 2006), and have been shown to be in good agreement on both a climatological and seasonal basis. Fishman et al. (2010) compared monthly average surface O_3 over central Indiana with TOR over a 5-year period and found a significantly positive correlation. Fishman et al. (1990)

compared monthly average   500-mb O_3 concentrations with TOR at several long-term ozonesonde sites and likewise found a strong positive correlation.
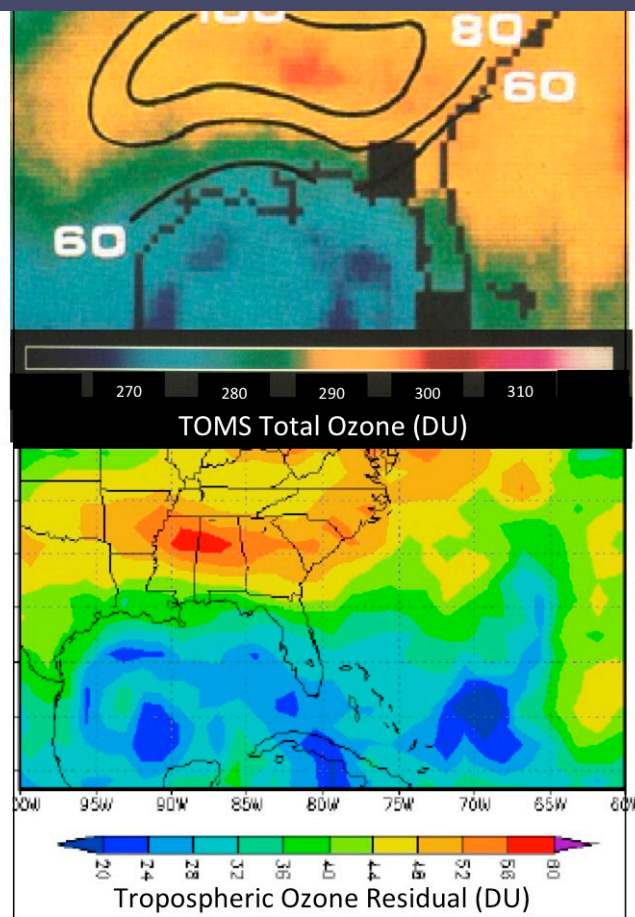
Within the next few years, TEMPO (Tropospheric Emissions: Monitoring of Pollution) will be launched in geostationary orbit.   By doing so, TEMPO, which, like OMI, GOME, and SCIAMACHY, also derives its information by applying a DOAS retrieval methodology to solar backscattered spectra, can make measurements on the order an hour (during daytime) and, by sitting in one location, gathers its information by "staring" over the entire United States (and parts of Mexico, Central America, and Canada), allowing it to provide measurements on scales of only few kilometers. However, despite the greatly enhanced spatial and temporal capability of TEMPO, no study has been conducted that relate these measurements to what may be measured at the surface.   The purpose of the research described herein is to provide an analysis of a regional photochemical-transport model simulation to study the relationship between quantities that will be measured by TEMPO to concentrations calculated at the surface for both ozone and NO_2.   Our study region is the greater St. Louis metropolitan area and we focus on the 5-day period of 1-5 July 2012, which was a time when the most ozone exceedances throughout the region were recorded over the past decade.

Our findings indicate that a well-defined plume of ozone throughout the lower troposphere can be simulated and related to a pollution episode at the surface.   The magnitude of this plume, however, is smaller than what had been shown to be present during widespread pollution episodes in the 1980s and may reflect on the successful implementation of U.S. emission controls over the past three decades.

1b. Previous Ozone Enhancements Observed by Satellites

Identification of enhanced total ozone column amounts were first published by Fishman et al. (1986) at tropical latitudes where the enhancements were associated with widespread biomass burning in the Brazilian cerrado, and, subsequently at middle latitudes in Fishman et al. (1987).   The enhancements found within the TOMS elevated integrated amounts over Brazil were consistent with the *in situ* aircraft profiles measured in a NCAR field campaign measured in 1980 (Crutzen et al., 1985).   Subsequent measurements from the TRACE-A field campaign (Fishman et al., 1996a;b) using ozonesonde, *in situ*, aircraft remotely sensed, and satellite measurements confirmed that enhancements in the TOMS total ozone signal were a result of widespread biomass burning over Brazil and southern Africa (Fishman et al., 1990), which, because of the low-level transport from the east and the upper-level transport from the west, highest TOR amounts were found over the south Atlantic Ocean.

During a widespread air pollution in August 1980, Fishman at al. (1987) showed that the extent of air pollution could be identified from an analysis of monitoring stations throughout much of the eastern U.S.   The top two panels in Figure 2 are taken from that study and illustrate how this synoptic-scale ozone pollution episode could be identified within the distribution of total ozone measurements obtained from TOMS instrument aboard the Nimbus 7 satellite.   The top panel depicts a vast area of the southeastern U.S., where daily maximum values   exceeded100 ppb at the surface.   To be included in this analysis, all stations involved in the analysis had been identified as not being directly downwind of an urban area.   This large area of elevated ozone at the surface ozone grew over a 4-day period as an intense anticyclone positioned itself over the eastern U.S. (Fishman and Balok, 1999).

Figure 2. Historical perspective of observing ozone pollution episode from surface analysis and satellite measurements. The top two panels are from Fishman et al. (1987) showing the surface analysis of a large scale ozone pollution episode and the total ozone distribution from TOMS over the southeastern U.S. The surface analysis in the top panel is superimposed on the TOMS measurements in the middle panel. The bottom panel is from Fishman et al. (2003) and shows the calculated TOR distribution from TOMS and SAGE measurements for August 8, 1980. The unusually low TOR values coincide with the presence of Hurricane Allen, a Category 5 storm that was moving slowly in the Gulf of Mexico on this day before making landfall in east Texas on 11 August. We speculate that clean tropical air was feeding into the storm resulting in low tropospheric ozone concentrations being present as air spiraled into the storm's center.

The bottom panel is the distribution of satellite-derived tropospheric ozone derived from the TOR technique described in Fishman et al. (2003), a modification of the initial TOR dataset described in Fishman et al. (1990). The spatial resolution of the satellite measurements (TOMS and SBUV) used to derive this distribution is on the order of 100 km. Since these instruments were aboard the polar-orbiting Nimbus-7 satellite, only one measurement per day is available. Despite this coarse spatial resolution, the satellite measurements were able to capture a feature of elevated surface ozone where the extent of this specific episode was on the order of 1000 km.

A second massive air pollution episode (Figure 3) enveloped much of the eastern U.S. occurred during the period of July 2-13 1988 (Fishman and Balok, 1999; Fishman et al., 2003). This case study (Schlichtel and Husar, 1998, private communication) was able to capture one of the most widespread ozone pollution episodes ever observed and stimulated studies of regional ozone pollution through the Ozone Assessment Transport Group (OTAG; Parker and Blodgett, 1999). As can be seen from the surface analysis, vast areas of the eastern U.S. exhibited surface concentration >90 ppb and later addressed in a reassessment of the surface ozone issue (NAS, 1991).
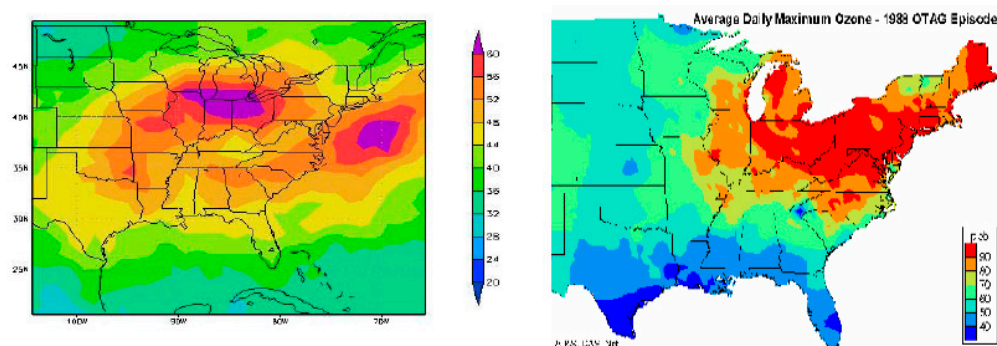
Figure 3. (left) Distribution of TOR during 2-13 July 1988 and the average daily ozone maximum for the same period (right). From Fishman et al. (2003) and Schlichtel and Husar (personal communication, 1998)

With the launch of TEMPO, which is planned for early next decade (~2020), the same kind of solar backscatter measurements described in the above studies (Fishman et al., 1986; 1987; Ziemke et al., 1998; 2006; 2014) will be obtained from a geostationary platform that continually views the continental U.S., thereby allowing for much better spatial (~4 km) and temporal (~1-hr) resolution during daylight hours (see discussion in Fishman et al., 2012; Zoogman et al. (2016). Although additional wavelengths in the visible part of the spectrum that covers the Chappuis Bands (centered at ~600 nm; Brasseur and Solomon, 1986, ch. 3) can provide some information in the lower troposphere that is more sensitive to the ozone in the boundary layer, the information in this region of the spectrum is still related to what is present in the entire column. The purpose of this study is to use a regional chemical/transport model to calculate column ozone amounts on this scale (~100 km) to see how they relate to the elevated O_3 concentrations measured at the surface.

II. RESULTS

### 2a. Model Description and Synoptic Situation

For analytical purposes, we use a model that can simulate the trace gases of interest at the same temporal and spatial resolution that would be observed from space by TEMPO. We used the Comprehensive Air quality Model with eXtensions (CAMx) to calculate the trace gas distributions discussed in this study. CAMx is an Eulerian regional photochemical dispersion model used to examine air pollution over many different scales ranging from neighborhoods to continents. The meteorological input for the model calculations described below were taken from simulations from the WRF (Weather Research and Forecasting) model (http://www.wrf-model.org/index.php), which was run with a 4-km resolution over our domain of interest, and which was embedded in a domain with a 12-km resolution bounded by 34°N to 44°N in the north-south direction and by 86°W to 96°W in the east-west direction, a region that includes all of Missouri, Illinois and Indiana and adjacent areas to both the north and south. The model was run from 20 June through 6 July and the last five days of that output was used as input for the calculations described in our case study. The day of greatest interest to us was July 2, 2012, which exhibited the highest concentrations of that summer, which was the most polluted summer of the decade between 2006 and 2016.

The CAMx model is built upon Fortran code and has binary input and output files that it uses in completing a run. During that specific period of this study, the temperature, wind speed and direction generated by WRF are consistent with what is often present for that time of year, as weak southwesterly winds prevailed in the St. Louis region of interest. Throughout the extended 10-day period from 28 June through 7 July, temperatures >37.8°C (100°F) were measured every day and record high temperatures were recorded for eight of those ten days in St. Louis. On a larger scale, the Midwest experienced considerably drier than average conditions; nationally, the July average

temperature was 25.3°C (77.6 °F), the warmest July and warmest month on record, dating back to 1895.

The surface map for 2 July at 1800Z (1300 CDT) is shown in Figure 4a.   Most of the region in the eastern U.S. is dominated by high pressure with a weak High identified in the Gulf of Mexico off the coast of Florida.   A weak frontal system is seen throughout the northern states, resulting in light, generally southwesterly, winds dominating the weather pattern in the St. Louis region.   As a result, with this typical summertime Bermuda High dominating much of the North American continent, precipitation formation was also inhibited and many afternoon thunderstorms that are often triggered by afternoon heating from the sun did not develop.

The occurrence of high ozone formation will likely occur when light winds and high temperatures are present with sufficiently high concentrations of NOx.   A map of the EPA Air Quality Index (AQI) for ozone is shown in Figure 4b.   Although the eastern U.S. is dominated by a situation conducive to the photochemical generation of high amounts of ozone, most of the region is characterized by only moderately high ozone concentrations.   A few pockets in the AQI "orange" (Unhealthy for sensitive groups; 71-85 ppb) range are present and a plume of elevated ozone is seen originating over the St. Louis urban area and transported by the prevailing southwesterly winds (insert of Fig. 4b).
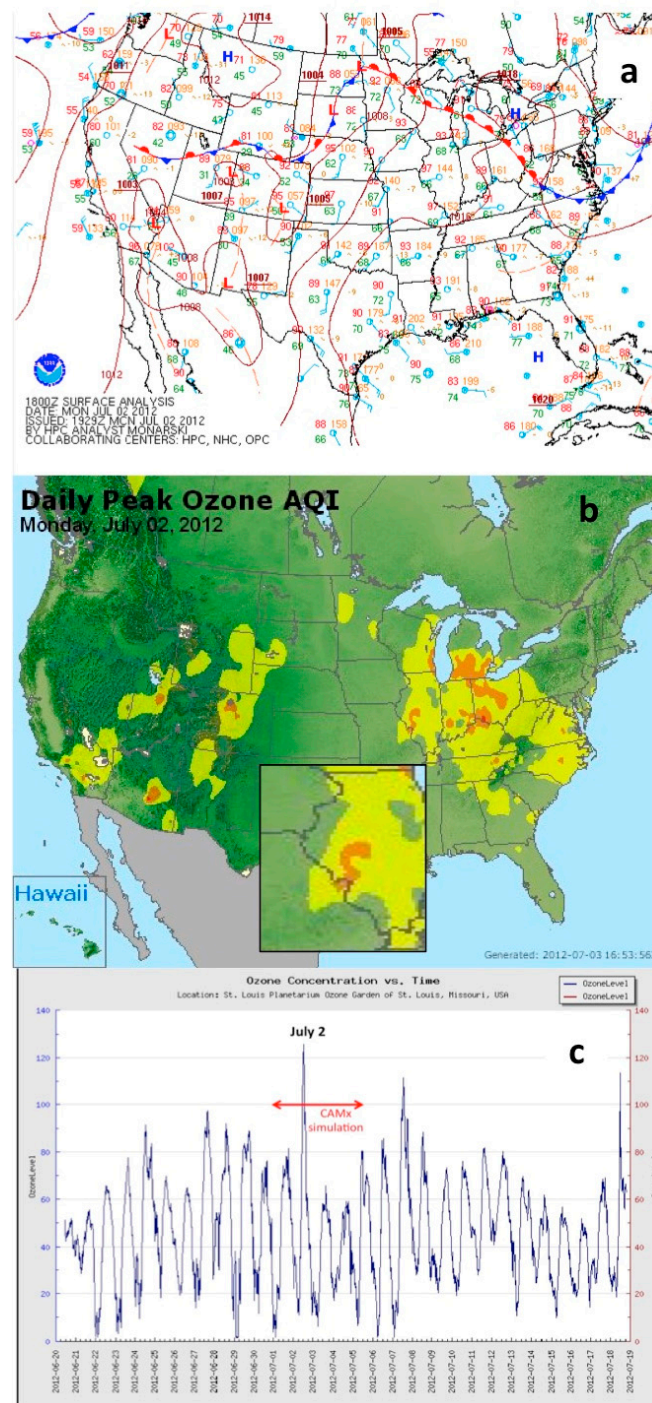
Figure 4 (a). HPC map showing July 2, 2012 at 1800 UTC (1:00 p.m CDT) surface analysis.   (b) AQI Ozone map for July 2, 2012.   Enlargement of the St. Louis region is inserted in the lower portion of this panel. (c) Ozone concentrations recorded at the St. Louis Planetarium between June 20 and July 7, 2012.   Also shown on this plot is the 5-day period when the CAMx model was run for this study. The highest O_3 concentration measured during the entire summer occurred on July 2nd.

From the end of June through much of July, the St. Louis Metropolitan Area experienced high ozone concentrations throughout the region.   All of these meteorological factors contributed to the high ozone concentrations experienced throughout much of the St. Louis region.   Figure 4c shows the ozone concentration between 20 June and 7 July 2012.   The period between June 27 and July 8, 2012, was the hottest 10-day period during the past decade where high temperatures exceeded 100°F every day and the daily maxima broke records on eight of those days.   High O_3 concentrations were

also measured for much of that period as shown in Figure 3c. The measurements depicted in this plot are taken from the St. Louis Ozone Garden (Fishman et al., 2014), located in Forest Park near the entrance of the McDonnell Planetarium. The monitor at this site records data every 15 minutes, whereas the AQS monitoring data has only a 1-hour time resolution. Also shown on this figure is the 5-day time period of the CAMx simulation and the concentration measured on July 2nd, which is when the site measured its highest concentration of the summer at 126 ppb.

2b. Simulation of Air Quality Parameters

From an air quality perspective, the most widely available dataset is the surface ozone measurements and we compare our model results with these observations. In general, there is reasonable agreement between the model-derived results and the observations, as is shown in Figure 5, which compares the average concentrations with AQS measurements during the 5-day model run. The solid lines are average concentrations taken from measurements eleven stations in the greater St. Louis region. The model calculations (dashed lines) capture the daily maximum concentrations reasonably well (within 5-10 ppb) for each of the days being simulated except on the 4 July, where the calculated maximum value is 88 ppb compared with an observed concentration of 60 ppb.
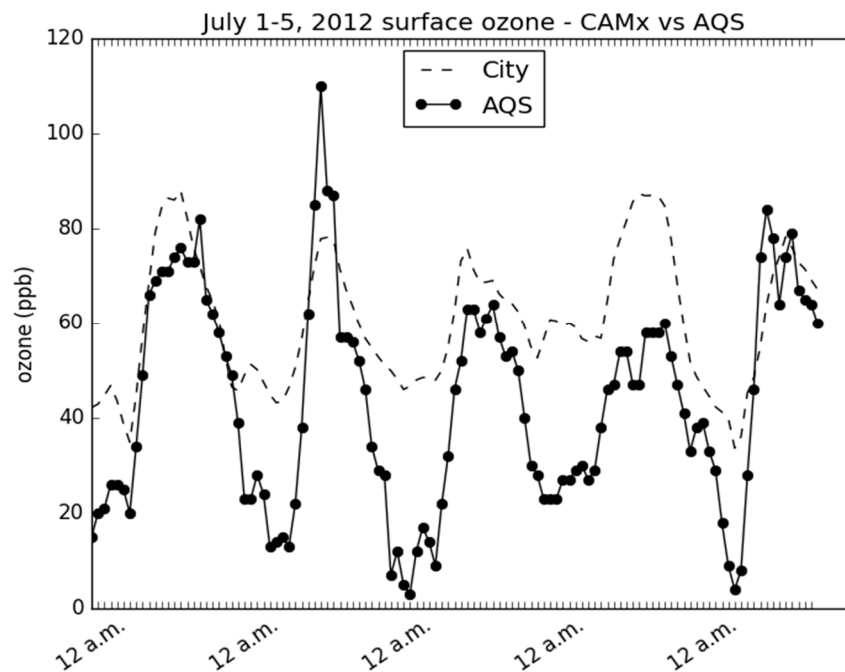

Figure 5. Solid line depicts the average O3 concentrations from the St. Louis AQS stations compared with the model-derived O3 concentrations (dashed line) during the period July 1-5, 2012.

Agreement between the calculations and the observations at night are not as good; model-derived surface concentrations are higher than what is observed. However, because this study is primarily concerned with comparing integrated daytime column amounts (when satellite measurements will be made) to surface concentrations, we feel that the daytime model simulations are reasonable for the discussion that follows. Furthermore, we are most interested in the daytime O3 concentrations since these values are the one that exceed that NAAQS criteria for a region being designated as one in nonattainment.

Figure 6 depicts the two-dimensional distribution of ozone at the surface during the day (July 2) at four different times as photochemical generation of ozone takes place. Lowest concentrations are visible in the morning (0600 LT) and are generally in the 35-40 ppb range near the city and surrounding environs. Highest concentrations are shown in the middle of the afternoon (1500 LT), with highest concentrations approaching 90 ppb, which is consistent with the depiction of the St. Louis plume shown in Figure 4b where "orange" AQI values denote a concentration of 71-85 ppb. These temporal and spatial patterns are consistent with the general observation that highest O_3 concentrations are found downwind of the urban area and that the surface plume identified in Figure 4b is well simulated by the model. Also depicted on these panels are three stars, which indicate representative locations upwind of the city, the center of the city, and downwind of the city.
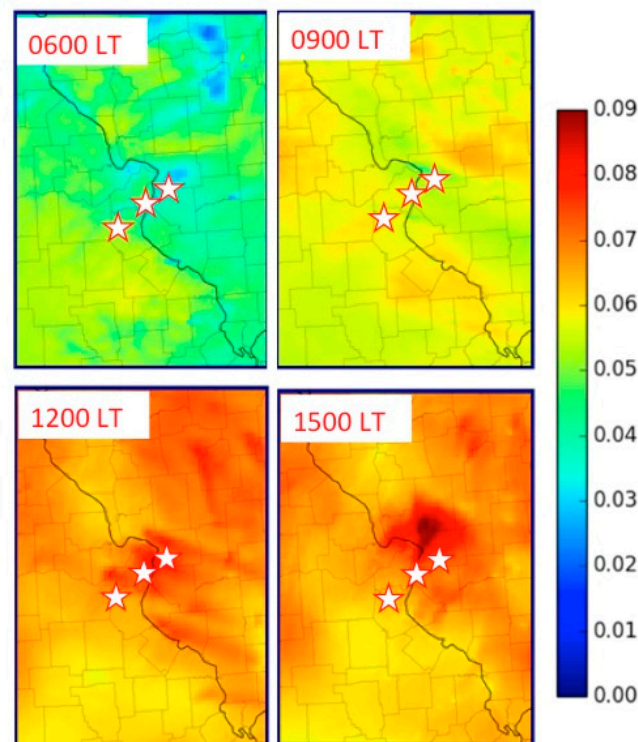

Figure 6. Evolution of the model-derived distribution of O_3 at the surface on July 2, 2012. The three stars show the locations of "upwind," "city," and "downwind" locations that will be discussed in more detail in the text and on subsequent figures.

Figure 7 compares the model-derived diurnal surface concentrations at the starred locations shown in Figure 6. Over the city, highest concentrations occur in the early afternoon (1200-1400 LT), whereas higher surface concentrations are found at the downwind location later in the afternoon (after 1300) and eventually peaking in the early evening. The upwind concentrations do not reach as high of a value as those found either over or downwind of the city during most hours.
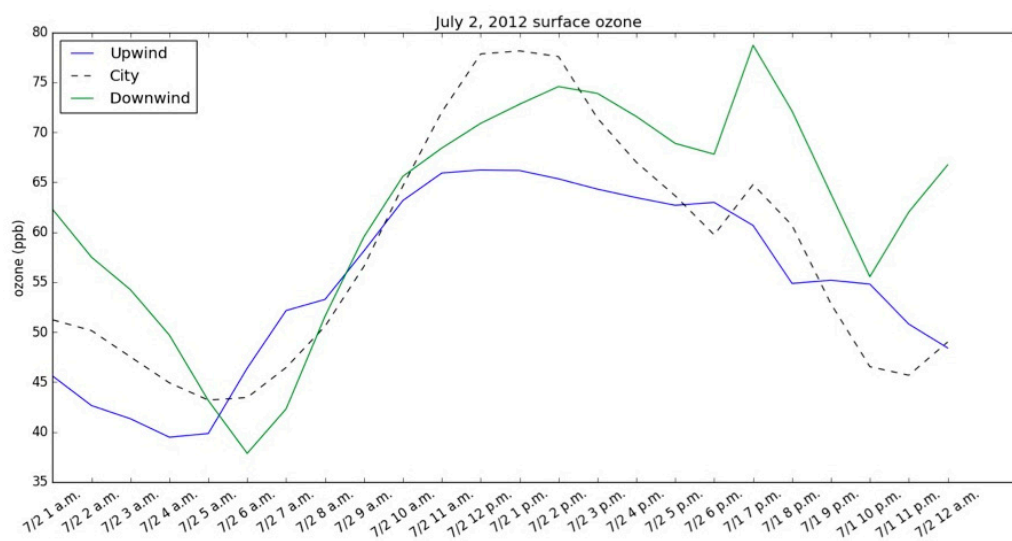
Figure 7. The diurnal concentrations of surface ozone at the upwind, city, and downwind locations shown in Figure 5.

Figure 8 shows model-derived ozone profiles in the lowest 10 km of the model at the three locations shown in Figure 6.   Throughout the course of the day, ozone builds up in the lowest layers of the model, generally to ~3 km and is transported with the prevailing light southwesterly winds. As a result of this transport, we find highest integrated ozone amounts ozone downwind of the city and later in the day relative to either the integrated amount over or upwind of the city.   Note that there is some variability in the ozone profiles above an altitude of 4 km, but because the air is less than half as dense in the middle and influences upper troposphere, the integrated amount of ozone between 4 and 10 km contributes only a relatively small fraction compared to how much the amount in the lowest 3-4 km contributes to the tropospheric column amount.
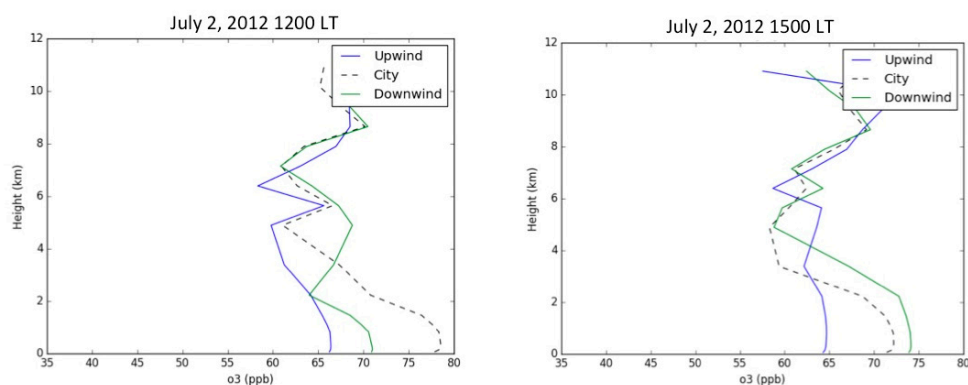
Figure 8.   Model-derived profiles of O_3 concentration from the surface to 12 km for the three locations shown in Figure 6.

Of particular interest in this modeling study are the depictions shown in Figure 9, illustrating how the integrated amount of tropospheric ozone (0-10 km) varies regionally over the course of a day (i.e., July 2).   Before the model photochemistry turns on with the rising sun, a very small gradient is found at 0600 LT.   As the daytime photochemistry develops, a well-defined urban plume is found downwind of the city.   This plume-like structure is more identifiable than what was calculated for the surface ozone concentrations shown in Figure 6.   Within the plume, integrated values as high as

4.2×10^{17} mol. cm^{-2} are at 1500 LT.   Integrated column amounts are commonly measured in Dobson Units (DU), where 1 DU = 2.69×10^{16} molecules cm^{-2}.   Thus, the plume emanating from St. Louis is ~16 DU, or only about one-third the magnitude of what was calculated from the TOMS/SBUV residual in the studies described in Fishman et al. (2003) and confirmed by aircraft measurements (Fishman et al., 1987).
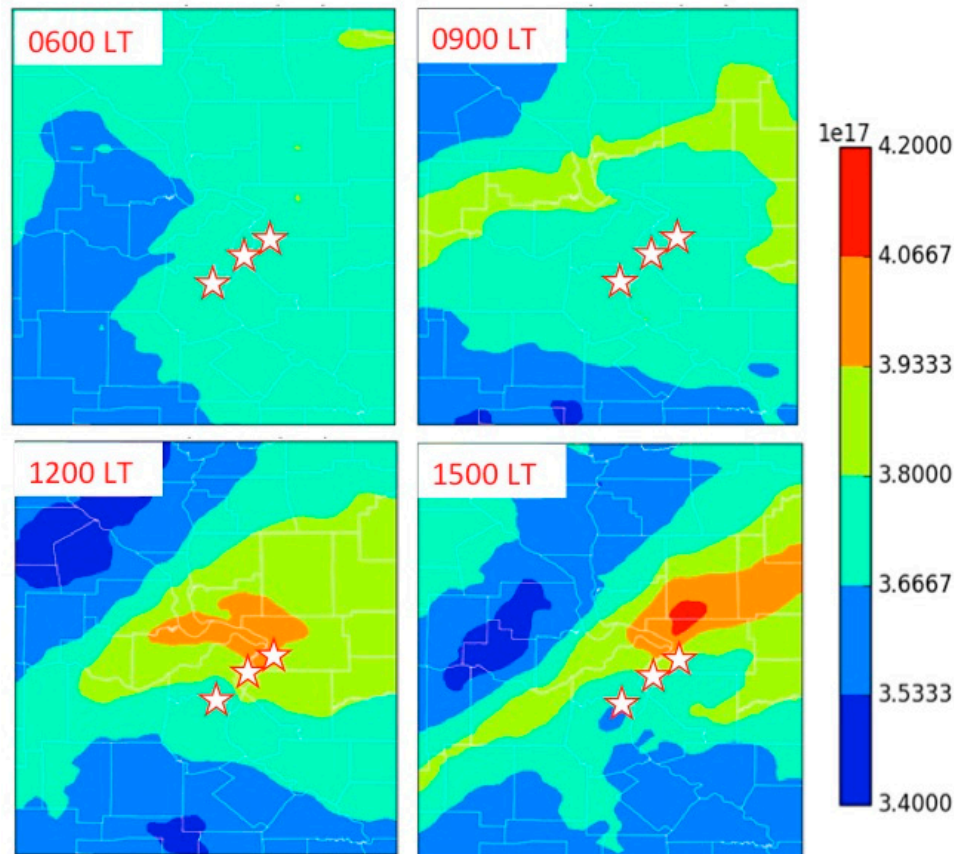

Figure 9.   The column integrated amount of ozone generated by the model for four different times of the day on July 2, 2012.

2c. Calculation of surface and integrated nitrogen dioxide

The atmospheric residence time of (NO$_2$) nitrogen dioxide is very short relative to other pollutants and goes through rapid conversion to nitric (NO) through photolysis.   However, because of the ubiquitous presence of ozone throughout the troposphere, the NO generated from NO$_2$ photolysis rapidly reacts with O$_3$ to put NO$_2$ back into the system.   This rapid interconversion reactions between NO, NO$_2$ and O$_3$ is often referred to as the photostationary state (Calvert, 1976). Figure 10a shows the calculated surface NO$_2$ concentrations at the three locations identified in Figure 6. As noted earlier, many of these concentrations are below the detection limit of routinely operating instruments, which have a detection lower limit of 1 ppb.
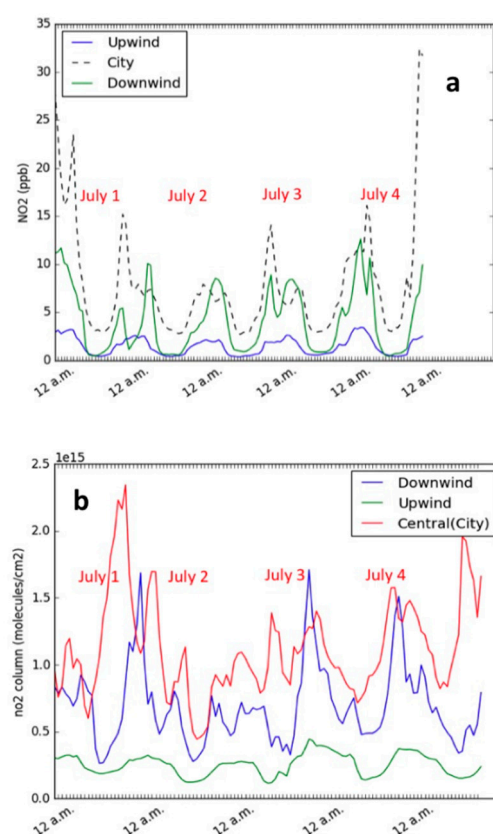
Figure 10(a) Model-derived surface NO_2 concentrations for the period July 1-5, 2012.   The three curves show the values at the three locations shown in Figure 6. (b) Model-derived integrated NO_2 concentrations for the period July 1-5, 2012.   The three curves show the values at the three locations shown in Figure 6.

The integrated amount of NO_2 over the period of the model run is shown in Figure 10b for each of the three locations in Figure 6.   The highest NO_2 integrals are generally found over the central city.   There are a few instances when the values downwind on a specific day exceed the amount over the city.   The day-to-day variability is dependent on a number of factors, including photochemistry, transport, and the daily pattern of the NO_x (primarily NO) emissions that increase considerably because of varying nature of vehicular emissions, which are highly correlated with rush-hour traffic. The concentrations at the upwind location are always lower than what is calculated over the city or downwind of it.

Background (i.e., upwind) integrated are calculated to be ~0.25 x 10^{15} mol. cm^{-2}, whereas urban values are generally 5-10 larger and can approach 2.5 x 10^{15} mol. cm^{-2}.   Such amounts are well above the threshold level for detection of NO_2 column amounts, but somewhat on the low end of values that have been measured over other urban areas (Cede et al., 2006).
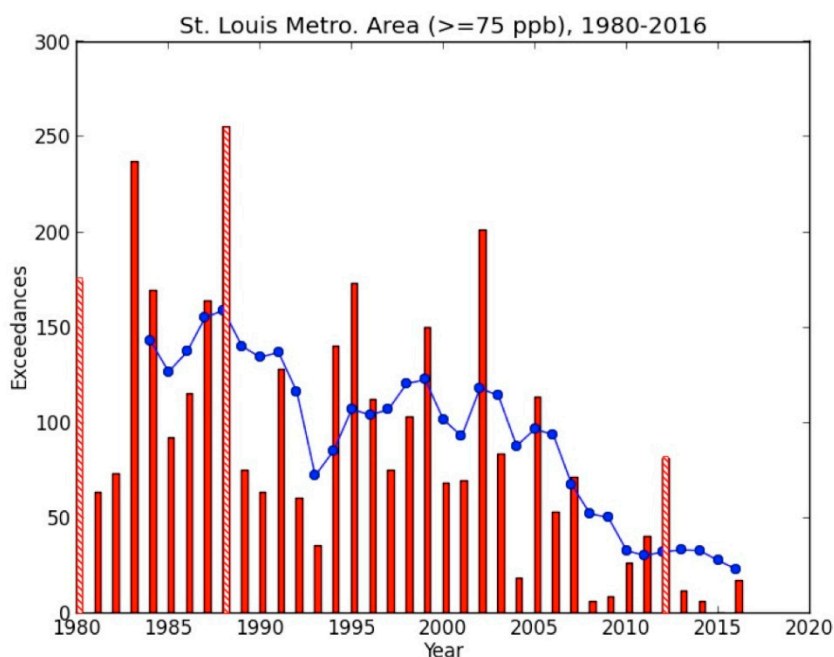
III. DISCUSSION

Using a reasonable simulation of a 5-day time period when elevated surface ozone concentrations above the NAAQS allowable criteria were present, the model calculations in this study show that integrated column amounts of ozone are likewise enhanced by as much as 20%.   The model also shows that integrated NO_2 column amounts are considerably larger, and can be as nearly ten times the amount calculated for locations upwind of the city, consistent with the early findings of Noxon (1979), who measured tropospheric column amount as low as 3 x 10^{14} mol. cm^{-2} in the mountains of Colorado and more than 5 x 10^{15} mol. cm^{-2} when the Denver plume passed over his

ground-based spectrometer.   In Cede et al. (2006), NO_2 column amounts of ~2 x 10^{16} mol. cm^{-2} have been measured in the greater Washington-Baltimore metropolitan area from OMI.

Our model-derived calculations show that total column amounts over and downwind of the St. Louis metropolitan area are generally are close to 2 x 10^{15} mol. cm^{-2}, which are on the order of 5-10 times larger than the amount calculated upwind.   These regional tropospheric enhancements are readily identifiable and have been reported in the literature on numerous occasions (e.g., Lamsal et al., 2008; 2014).

Detection of regional-scale outbreaks of an ozone episode may prove more challenging now than when the NAAQS standards were first developed in the 1970s.   Figure 11 depicts the number of exceedances over the St. Louis region between 1980 and 2016.   The number of exceedances per year is the criterion that determines whether or not a specific region is in violation of the NAAQS for ozone.   When these standards were first released they were based on concentrations over a 1-hr period.   In 1999, the NAAQS was redefined using an 8-hr standard as research showed that a longer exposure to high ozone at elevated concentrations was more damaging to human health than the relatively shorter (1-hr) exposure time, even at higher concentrations (125 ppb) for a given hour, which was the original NAAQS standard.   We have reanalyzed the measurements available from the St. Louis metropolitan AQS monitoring system and have produced the data shown in Figure 11 by summing the number of times any monitoring site in the network reached an 8-hr maximum concentration of 75 ppb or greater.   Over the years, ~10 monitors have operated in the greater St. Louis region, which includes sites in both Missouri and Illinois.   Because of the implementation of emission controls, the number of exceedances has decreased considerably between 1980 and 2016. It should be noted, however, that only three or four stations were in operation in 1980, the first year of data we were able to obtain.   Thus, it is likely that the number of exceedances would have been much higher (possibly by a factor of 2 to 3) had the data been analyzed from ten or so monitors.   The years in which examples have been discussed in this study (1980, 1988, and 2012) are designated by red hatching.   The National Academy of Science (NAS, 1991) provided a report on the widespread nature of ozone episodes, such as those shown here in the case studies of 1980 and 1988 and noted how the year-to-year variability was dependent of prevailing meteorological conditions.   In particular EPA (2004) notes that the years 1980, 1983 and 1988 were the years of highest concentrations between 1979 and 2003.

Figure 11. The number of exceedances (red bars) over the metropolitan St. Louis region using the 2008 8-hr standard (75 ppb) for each year.   The hatched bars (1980, 1988, and 2012) are years in which regional examples are discussed in the text.   During most years, there were generally ~10 stations providing measurements.   During 1980, however, the first year of measurements analyzed, only three stations operated.   If ten stations would have been providing data, the number of exceedances would have been considerably higher.   Ozone trends data from 1980 through 2010 summarized in EPA (2012) shows that U.S. ozone concentrations were highest during the summers of 1988, 1983, and 1980, in that order.   The blue line is the 5-year running average of the number of exceedances.

Over the past decade of observations, the summer of 2012 was the most polluted year in St. Louis in terms of the number of exceedances.   There is generally a strong correlation between summertime temperatures and ozone and 2012 was the hottest year on record in St. Louis since 1954, or, in other words, since routine pollution monitoring had been in existence.   Thus, despite the record heat, U.S. regional emission controls, especially those for NO_2 implemented in 2005, suggest that ozone pollution has been greatly reduced (see Duncan et al., 2016).

The model calculations in this paper calculate a regional enhancement of ~30 ppb during an episode where many exceedances occur, i.e., ~90 ppb as a maximum, where background daytime concentrations are on the order of 60 ppb (see Figure 6, depiction at 1500 LT and Fishman et al., 2010). These ozone-plume enhancements are consistent with what was observed by the monitoring network in the St. Louis area.   When this enhancement is primarily confined to the lowest 3 km of the model's vertical domain, it corresponds to an increase of ~0.6 x 10^{17} mol. cm^{-2}, or ~2-3 DU, compared to values outside of plume.   On the other hand, the emissions coming from St. Louis are considerably smaller to what is emitted by other cities in the eastern U.S.

As a background to this study, we showed that widespread synoptic-scale pollution episodes covered the eastern U.S. in the 1980s, and identified two specific synoptic-scale (hundreds of km) episodes in 1980 and 1988.   Examination of aircraft measurements from the UV-DIAL (Ultraviolet Differential Airborne Lidar) system aboard a NASA research aircraft taking measurements in the PEPE/NEROS (Persistent Elevated Plume Episode/NorthEast Regional Oxidant Study) found enhanced ozone concentrations >110 ppb over a domain that stretched ~300 km up to an altitude of 1 km (Fishman et al., 1987).   Such an episode generates an enriched airmass of ozone on the order of containing 16-24 DU over a scale of several hundred km, and the magnitude of this event was identifiable from the relatively crude satellite instruments that were in orbit in the 1980s.   Through the implementation of emission controls over the past several decades, the presence of air pollution

episodes on such a massive scale have been virtually eliminated.   As shown by our calculations, the enhancements seen on the regional scale are only on the order of 12-15 DU for St. Louis, and only ~6 DU above the values calculated for the background concentrations.   For St. Louis, in particular in this study, the plume of elevated ozone extends on the order of less than 100 km, considerably smaller in scale that those identified previously in 1980 and 1988.   Because the stratospheric overburden during the summer at northern middle latitudes is on the order of 300 DU, the enhancement in the amount of ozone generated in the boundary layer (i.e., the lowest 3 km) is going to be considerably more difficult to isolate.

Returning to the AQI depiction shown for July 2, 2012, in Figure 3b, virtually no "red" ($O_3 > 85$ ppb) areas are found in the eastern U.S.   Going through the Airnow archive, which dates going back through 2012, the presence of areas depicted in red ("unhealthy"; $O_3 > 86$ ppb), are quite uncommon, and when present never have the areal extent as the ones shown in the surface analysis in Figures 3 and 4, where the red values in that panel indicate concentrations of 90 ppb or more.   During the episode shown in Figure 2, continuous ozone profile measurements using the UV-DIAL (Browell et al., 1985) system made measurements on August 7, 1980 (the day before the depictions shown in Figure 2) in the Pennsylvania and Ohio as part of the PEPE/NEROS (Persistent Elevated Pollution Episode/Northeast Regional Oxidant Study).   In terms of high ozone concentrations, this region was not as polluted as the pollution in the southeast on the following day, as shown in the top panel, but concentrations as high as 110 ppb extended for a distance of more than 300 km and reached a vertical depth of more than 1000 m with concentrations of 90 ppb reaching as high as 1.5 km along the flight path (Fishman et al., 1987).   When integrated along the flight path, integrated ozone column amounts ranged between 15 and 20 DU (4.0×10^{17} to 5.4×10^{17} mol. cm^{-2}).   Although it is difficult to provide a definitive quantitative estimate comparing the pollution episodes identified in 1980 and 1988 with the modeling study presented here, it is clear that the magnitude and the spatial extent of the situation modeled in this study are considerably less, at least in qualitative terms.   The conclusion we draw from our model calculations and from a qualitative analysis of the ozone pollution episodes during 2012 and subsequent years is that there has been a significant reduction in ozone pollution in the past decade compared to what had occurred in the 1980s.   Although this is good news for air quality managers, it points to the fact that the capability of trying to observe present-day and future pollution events once TEMPO is launched is going to present a greater challenge than if the satellite had been launched in the 1980s.

IV. SUMMARY AND CONCLUSIONS

Through the use of a regional photochemical/transport model, we have discussed the simulated ozone and nitrogen dioxides distributions during an air pollution in the greater St. Louis region, July 1-5, 2012.   The model was then used to determine the surface concentrations and integrated tropospheric amount of these trace species.   The surface ozone observations are in reasonable agreement with the model results and confirm the calculations that higher ozone concentrations are found downwind of the city.

Surface NO_2 concentrations are highest over the city, consistent with other analyses of satellite measurements (Cede et al., 2006).   The integrated gradients calculated by the model show gradients where values generally differ by a factor of 4 to 5, consistent with other observations from satellites and should readily observable from space.

The St. Louis plume generated by the model show an enhancement of ozone emanating from the source region, as expected.   The magnitude of this plume maximizes at 15 DU and a discernable enhancement relative to surrounding nonurban environs is ~6 DU, and is considerably smaller in extent than the pollution episodes over the eastern U.S. in 1980 and 1988.   Thus, there should be identifiable plumes of ozone that could be measured by TEMPO, but their smaller magnitude make their being observable by TEMPO more challenging than when such plumes were generated in the 1980s before 21st-century emission controls were implemented.

Lastly, the relative lack of the presence of the large ozone pollution episodes that were more prevalent during the 1980s might be indicative of a trend for the entire eastern U.S.   Examination of

the daily ozone AQI maps since 2012 show only sparse amounts of "unhealthy" (i.e., red; 8-hr concentrations >85 ppb) throughout the eastern U.S. implying daily average concentrations nearly everywhere nearly every summer day are less than 85 ppb. Although the surface concentrations shown during the pollution episodes reflect daytime hourly maximum values, it is likely than many of the red areas and contours >100 ppb in figures 4 and 5 would have likewise shown up as "red" under the AQI criteria. However, we do acknowledge that a more rigorous analysis must be carried out to verify this anecdotal hypothesis. The scientific community through the International Global Atmospheric Chemistry (IGAC) Project is in the final stages of completing a comprehensive assessment of tropospheric ozone through ITS TOAR (Tropospheric Ozone Assessment Report) initiative (http://www.igacproject.org/sites/default/files/2017-02/TOAR_overview_0.pdf). It is likely that the results of this study will find the paradoxical analysis that ozone generated from pollution episodes is decreasing in the eastern   U.S. while concurrently concluding that background concentrations are increasing due to long range transport from across the Pacific, which would make the prospect of keeping ozone standards below EPA guidelines an even greater challenge (Fishman et al., 2014), especially if the NAAQS standard is lowered, as currently proposed.

Figure Captions: Figure 1. Comparison of satellite-derived and bottoms-up emissions estimates (from Lu et al., 2015)

Figure 2.   Historical perspective of observing ozone pollution episode from surface analysis and satellite measurements. The top two panels are from Fishman et al. (1987) showing the surface analysis of a large scale ozone pollution episode and the total ozone distribution from TOMS over the southeastern U.S. The surface analysis in the top panel is superimposed on the TOMS measurements in the middle panel. The bottom panel is from Fishman et al. (2003) and shows the calculated TOR distribution from TOMS and SAGE measurements for August 8, 1980. The unusually low TOR values coincide with the presence of Hurricane Allen, a Category 5 storm that was moving slowly in the Gulf of Mexico on this day before making landfall in east Texas on 11 August. We speculate that clean tropical air was feeding into the storm resulting in low tropospheric ozone concentrations being present as air spiraled into the storm's center.

Figure 3. (left) Distribution of TOR during 2-13 July 1988 and the average daily ozone maximum for the same period (right). From Fishman et al. (2003) and Schlichtel and Husar (personal communication, 1998)

Figure 4 (a). HPC map showing July 2, 2012 at 1800 UTC (1:00 p.m CDT) surface analysis.   (b) AQI Ozone map for July 2, 2012. Enlargement of St. Louis region is   shown in the lower right of this panel. (c) Ozone concentrations recorded at the St. Louis Planetarium between June 20 and July 7, 2012. Also shown on this plot is the 5-day period when the CAMx model was run for this study. The highest O3 concentration measured during the entire summer occurred on July 2nd.

Figure 5. Solid line depicts the average O3 concentrations from the St. Louis AQS stations compared with the model-derived O3 concentrations (dashed line) during the period July 1-5, 2012.

Figure 6. Evolution of the model-derived distribution of O3 at the surface on July 2, 2012. The three stars show the locations of "upwind," "city," and "downwind" locations that will be discussed in more detail in the text and on subsequent figures.

Figure 8.   Model-derived profiles of O3 concentration from the surface to 12 km for the three locations shown in Figure 6.

Figure 9.   The column integrated amount of ozone generated by the model for four different times of the day on July 2, 2012.

Figure 10(a) Model-derived surface NO2 concentrations for the period July 1-5, 2012. The three curves show the values at the three locations shown in Figure 6. (b) Model-derived integrated NO2 concentrations for the period July 1-5, 2012. The three curves show the values at the three locations shown in Figure 6.

Figure 11.   The number of exceedances (red bars) over the metropolitan St. Louis region using the 2008 8-hr standard (75 ppb) for each year.   The hatched bars (1980, 1988, and 2012) are years in which regional examples are discussed in the text.   During most years, there were generally ~10 stations providing measurements.   During 1980, however, the first year of measurements analyzed, only three stations operated.   If ten stations would have been providing data, the number of exceedances would have been considerably higher.   Ozone trends data from 1980 through 2010 summarized in EPA (2012) shows that U.S. ozone concentrations were highest during the summers of 1988, 1983, and 1980, in that order.   The blue line is the 5-year running average of the number of exceedences.

References

1.   Browell, E.V.; Carter, A.F.; Shipley, S.T.; Allen, R.J.; Butler, C.F.; Mayo M.N.; Siviter, J.H.; and Hall, W.M., NASA multipurpose airborne DIAL system and measurements of ozone and aerosol profiles, *Appl. Opt,,* **1985,** *22,* 522-534.

2.   Brasseur G.; and Solomon, S. *Aeronomy of the Middle Atmosphere (2nd ed.)*, Reidel, Dordrecht, Holland, 1986, pp. 144-157.

3.   Calvert, J.G. Test of the theory of ozone generation in Los Angeles atmosphere. *Env. Sci. Tech.*, **1976**. *10*, 248-262.

4.   Cede, A.; Herman, J.; Richter, A.; Krotkov, N.; Burrows, J. Measurements of nitrogen dioxide total column amounts using a Brewer double spectrophotometer in direct Sun mode, *J. Geophys. Res.,* **2006**, *111*, D05304, doi:10.1029/2005JD006585.

5.   Crutzen, P. J.;. Delany, A.C.; Greenberg, J.;Haagenson, P.; Heidt, L.; Lueb, R.; Pollock, W.; Seiler, W.; Wartburg A.; Zimmerman, P. Tropospheric chemical composition measurements in Brazil during the dry season, . *Atmos. Chem*., **1985**, *2*, 233-256.

6.   Duncan, B.N., et al. (25 authors).   Satellite Data of Atmospheric Pollution for U.S. Air Quality Applications: Examples of Applications, Summary of Data End-User Resources, Answers to FAQs, and Common Mistakes to Avoid, *Atmos. Environ.,* **2016**, doi:10.1016/j.atmosenv.2014.05.061.

7.   EPA, The Ozone Report: Measuring Progress through 2003, U.S. EPA 454/K-04-001, April 2004, Research Triangle Park NC, 23pp. (Available on line at: https://nepis.epa.gov/Exe/ZyNET.exe/10004DTX.txt?ZyActionD=ZyDocument&Client=EPA&Index=2000 %20Thru%202005&Docs=&Query=&Time=&EndTime=&SearchMethod=1&TocRestrict=n&Toc=&TocEntr y=&QField=&QFieldYear=&QFieldMonth=&QFieldDay=&UseQField=&IntQFieldOp=0&ExtQFieldOp=0 &XmlQuery=&File=D%3A%5CZYFILES%5CINDEX%20DATA%5C00THRU05%5CTXT%5C00000008%5 C10004DTX.txt&User=ANONYMOUS&Password=anonymous&SortMethod=h%7C- &MaximumDocuments=1&FuzzyDegree=0&ImageQuality=r75g8/r75g8/x150y150g16/i425&Display=hpfr &DefSeekPage=x&SearchBack=ZyActionL&Back=ZyActionS&BackDesc=Results%20page&MaximumPag es=1&ZyEntry=2)

8.   Fishman, J.; Balok, A.E. Calculation of Daily Tropospheric Ozone Residuals Using TOMS and Empirically-Improved SBUV Measurements: Application to an Ozone Pollution Episode over the Eastern United States, *J. Geophys. Res.,* **1999**, *104*, 30,319-30,340.

9.   Fishman, J.; Minnis, P.; Reichle, Jr., H. G.: The Use of Satellite Data to Study Trace Gas Emissions in the Tropics. *J. Geophys. Res.*, **1986**, *91*, No. D13, 14451-14465.

10. Fishman, J.; Vukovich, F. M.; Cahoon, D. R.; and Shipham, M. C. The Characterization of an Air Pollution Episode Using Satellite Total Ozone Measurements*.   J. Clim. Appl. Meteor*. **1987**, *26*, 1623-1654.

11. Fishman, J.; Hoell, Jr., J.M.; Bendura, R.D.; Kirchhoff, V.W.J.H.; McNeal, R.J. The NASA GTE TRACE-A Experiment (September-October, 1992), *J. Geophys. Res.,* **1996a** *101*, D19, 23,865-23,879.

12. Fishman, J.; Brackett, V.G.; Browell, E.V.; Grant, W.B. Tropospheric Ozone Derived from TOMS/SBUV Measurements during TRACE-A, *J. Geophys. Res.* **1996b,** *101,* 24,069-24,082.

13. Fishman, J.; Wozniak, A.E.; Creilson, J.K. Global distribution of tropospheric ozone from satellite measurements using the empirically corrected tropospheric ozone residual technique: Identification of the regional aspects of air pollution, *Atmos. Chem. Phys.,* **2003,** *3, * 893-907, (www.atmos-chem-phys.org/acp/3/893/).

14. Fishman, J.; Creilson, J.K.; Parker, P.A.; Ainsworth, E.A.; Vining, G.G.; Szarka, J.; Booker, F.L.; Xu, X. An investigation of widespread ozone damage to the soybean crop in the upper Midwest determined from ground-based and satellite measurements, *Atmos. Environ.* **2010,** doi:10.1016/jatmosenv.2010.01.015.

15. Fishman, J.; Belina, K.M.; Encarnaciòn, C.H The St. Louis Ozone Gardens: Visualizing the impact of a changing atmosphere, *Bull. Amer. Meteor. Soc.,* **2014**, *85,*1171-1176.

16. Lamsal, L.N., Martin, R.V., Steinbacher, M., Celarier, E. A., Bucsela, E., Dunlea, E. J., and Pinto, J.: Ground level nitrogen dioxide concentrations inferred from the satellite-borne Ozone Monitoring Instrument, *J. Geophys. Res.,* **2008,***113*, 35 doi:10:1029/2007DJ009235.

17. Lamsal, L. N., Krotkov, N. A., Celarier, E. A., Swartz, W. H., Pickering, K. E., Bucsela, E. J., Gleason, J. F., Martin, R. V., Philip, S., Irie, H., Cede, A., Herman, J., Weinheimer, A., Szykman, J. J., and Knepp, T. N.: Evaluation of OMI operational standard NO2 column retrievals using in situ and surface-based NO2 observations, *Atmos. Chem. Phys.,* **2014,** *14*, 11587–11609,

18. Levelt, P. et al. (44 co-authors) The Ozone Monitoring Instrument: Overview of twelve years in space, *Atmos. Chem. Phys. Disc.* **2017** *(*https://doi.org/10.5194/acp-2017-487)

19. Lu, Z.; Streets, D. G.; de Foy, B.; Lamsal, L. N.; Duncan, B.N.; Xing, X. Emissions of nitrogen oxides from US urban areas: estimation from Ozone Monitoring Instrument retrievals for 2005-2014, *Atmos. Chem. Phys.,* **2015,***15*, 10367-10383,

20. NAS *Rethinking the Ozone Problem in Urban and Regional Air Pollution*, National Academies Press, Washington DC, 1991,524 pp. (pdf available at http://www.nap.edu/catalog/1889.html.)

21. Parker, L., and J. Blodgett (1999), Air Quality: EPA's Ozone Transport Rule, OTAG, and Section 126 Petitions -- A Hazy Situation? (available from National Digital Library, retrieved July 2017) (https://digital.library.unt.edu/ark:/67531/metacrs935/m1/1/high_res_d/98-236_1999Jun15.html#Back4)

22. Platt, U., and J. Stutz (2008). *Differential Optical Absorption Spectroscopy*. *Springer*, Berlin, Germany, 597 pp.

23. Russell, A.R.; Valin, L. C.; Cohen, R.C. Trends in OMI NO2 observations over the United States: effects of emission control technology and the economic recession, A*tmos. Chem. Phys.,* 2012, *12*, 12197–12209, ,www.atmos-chem-phys.net/12/12197/2012/ doi:10.5194/acp-12-12197-2012

24. Ziemke, J. R.; Chandra, S.; and Bhartia, P. K.: Two new methods for deriving tropospheric column ozone from TOMS 35 measurements: The assimilated UARS MLS/HALOE and convective-cloud differential techniques, *J. Geophys. Res.,* *103*, 1998, doi:10.1029/98JD01567, 22,115-22,127,.

25. Ziemke, J. R.; Chandra, S.; Duncan, B. N.; Froidevaux, L.; Bhartia, P. K.; Levelt, P. F.; Waters, J. W. Tropospheric ozone determined from Aura OMI and MLS: Evaluation of measurements and comparison with the Global Modeling Initiative's Chemical Transport Model, *J. Geophys. Res.,* 2006, *111*, D19303, doi:10.1029/2006JD007089,.

26. Ziemke, J. R.; Olsen, M. A.; Witte, J. C.; Douglass, A. R.; Strahan, S. E.; Wargan, K.; Liu, X.; Schoeberl, M. R.; Yang, K.; Kaplan, T. B,; Pawson, S.; Duncan, B. N.; Newman, P. A.; Bhartia, P. K.; Heney, M. K. Assessment and applications of NASA ozone data products derived from Aura OMI/MLS satellite measurements in context of the GMI Chemical Transport Model, *J. Geophys. Res.,* **2014**, *119,* 5671-5699, doi:10.1002/2013JD020914,.

27. Zoogman, P., et al. (39 co-authors), Tropospheric Emissions: Monitoring of Pollution (TEMPO), *J. Quant. Spectroscopy Rad. Transfer,* **2017**, *186*, (in press) (http://dx.doi.org/10.1016/j.jqsrt.2016.05.008)